



Research article

Dapagliflozin ameliorates myocardial infarction injury through AMPK α -dependent regulation of oxidative stress and apoptosis

Yuce Peng^{a,c,1}, Mingyu Guo^{a,c,1}, Minghao Luo^{a,c}, Dingyi Lv^{a,c}, Ke Liao^{a,c},
Suxin Luo^{a,c,**}, Bingyu Zhang^{a,b,*}

^a Department of Cardiology, The First Affiliated Hospital of Chongqing Medical University, Chongqing, 400016, China

^b Department of Cardiology, Wuhu Hospital of East China Normal University, Wuhu, China

^c Cardiovascular Disease Laboratory of Chongqing Medical University, Chongqing, 400016, China

ARTICLE INFO

Keywords:

Myocardial infarction
Dapagliflozin
Oxidative stress
AMPK α
Apoptosis

ABSTRACT

Dapagliflozin (DAPA) has been demonstrated to reduce cardiovascular mortality and heart failure hospitalization rates in diabetic patients. However, the mechanism underlying its cardio-protective effect in non-diabetic patients remains unclear. Our study aimed to explore the cardio-protective impact of DAPA on myocardial infarction in non-diabetic mice. We induced myocardial infarction in C57BL/6 mice by ligating the descending branch of the left coronary artery. After surgery, the animals were randomly treated with either saline or DAPA. We employed echocardiography, Western blot analysis, and tissue staining to assess post-infarction myocardial injury. Additionally, we investigated the mechanism of action through cell experiments. Compared to the myocardial infarction group, DAPA treatment significantly attenuated ventricular remodeling and improved cardiac function. By mitigating myocardial oxidative stress and apoptosis, DAPA may activate the AMPK α signaling pathway, thereby exerting a protective effect. These findings suggest that DAPA could serve as a novel therapeutic approach for patients with cardiac infarction.

1. Introduction

Myocardial infarction (MI) is usually caused by an acute interruption of coronary blood flow due to plaque shedding and a series of changes in cardiac structure and function, ultimately leading to irreversible death of cardiomyocytes and impaired cardiac function [1]. Although timely implementation of reperfusion strategies reduces acute myocardial infarction-related mortality, cardiomyocytes have little regenerative capacity, making MI and its sequelae remain the leading cause of death worldwide [2]. Therefore, alleviating the death of cardiomyocytes would be an effective way to treat myocardial infarction and promote recovery. Recent studies have shown that myocardial infarction leads to the release of numerous inflammatory mediators and increased production of reactive oxygen species (ROS). ROS can oxidize lipids, proteins, and DNA because of its high reactivity [3], leading to changes in cell structure and function, causing cardiomyocyte apoptosis, aggravating cardiac insufficiency, and even causing heart failure. ROS is closely related to the progression of cardiovascular disease [4]. It is challenging to improve cardiac function, reduce mortality and better

* Corresponding author. Department of Cardiology, The First Affiliated Hospital of Chongqing Medical University, Chongqing, 400016, China.

** Corresponding author. Department of Cardiology, The First Affiliated Hospital of Chongqing Medical University, Chongqing, 400016, China.

E-mail addresses: luosuxin@hospital.cqmu.edu.cn (S. Luo), Zhangbingyu81@126.com (B. Zhang).

¹ Those authors contribute equally to this work.

<https://doi.org/10.1016/j.heliyon.2024.e29160>

Received 13 April 2023; Received in revised form 31 March 2024; Accepted 2 April 2024

Available online 4 April 2024

2405-8440/© 2024 Published by Elsevier Ltd.

This is an open access article under the CC BY-NC-ND license

(<http://creativecommons.org/licenses/by-nc-nd/4.0/>).

outcomes after myocardial infarction.

Currently, sodium-glucose cotransporter 2 (SGLT2) inhibitors are the latest treatment for heart failure of type 2 diabetes, which could lower blood sugar in diabetic patients by inhibiting renal SGLT2 and reducing glucose reabsorption [5,6]. Clinical trials have shown that SGLT2 inhibitors can significantly reduce cardiovascular mortality and heart failure hospitalization in patients with type 2 diabetes, revealing its cardiovascular protective effect in diabetic patients [7–9]. The study by Chenguang Li et al. showed that DAPA could improve the structure and function of diabetic myocardium by inhibiting the transforming growth factor β /SMAD pathway [10, 11]. Interestingly, studies have pointed out that DAPA could significantly decrease the risk of worsening HF or cardiac death in HF patients with a reduced ejection fraction, regardless of the presence or absence of diabetes [12], suggesting that its protective effect on the heart is independent of the mechanism of lowering glucose. SGLT2 inhibitors confer cardioprotective effects by inhibiting cardiomyocyte autosis (autophagic cell death) regardless of diabetes as well as mediating M2 polarization through a ROS-dependent STAT3-mediated pathway [13,14].

Although cardiomyocytes do not express SGLT2, the precise protective mechanism of DAPA in the hearts of non-diabetic patients remains to be fully understood. Therefore, we conducted this study to investigate the impact of the SGLT2 inhibitor DAPA on cardiac function following non-diabetic myocardial infarction and explore the underlying mechanisms.

2. Materials and methods

2.1. Ethical approval and experimental animals

All experimental procedures conformed with the National Institutes of Health Guidelines for the Use of Laboratory Animals and were approved by The Chongqing Medical University Animal Research Committee (ethical approval number: IACUC-CQMU-2023-0082). Adult healthy male C57 mice, weight 20–25 g, were purchased from Shanghai Model Organisms Center. Mice were bred in Chongqing Medical University animal experiment center at a temperature of $26\text{ }^{\circ}\text{C} \pm 2\text{ }^{\circ}\text{C}$, relative humidity of $50\% \pm 15\%$, and a programmed 12-h light/12-h dark cycle for circadian control. All the mice got free water and food. As usual, these animals were fed with standard chow and water for one week before any operative procedures.

2.2. Establishment of AMI models and treatments

After a week of acclimatization, mice were randomly divided into 4 groups with 12 mice in each group. (1) the Sham group: mice with sham operation treated with phosphate buffer saline (PBS) (Sham), (2) Sham + DAPA group: mice with sham operation treated with DAPA (1 mg/kg per day, MCE, HY-10450, dissolved in PBS) (Sham + DAPA), (3) Myocardial Infarction (MI) group: MI mice treated with Phosphate buffered saline (PBS) (MI), and (4) MI + DAPA group: MI mice treated with DAPA (MI + DAPA). Due to postoperative death and other conditions, we randomly selected 6 mice in each group for the subsequent experiment.

Mice myocardial infarction models were induced by left anterior descending (LAD) ligation. Briefly, mice were fasted for 12 h and then anesthetized with isoflurane inhalation(3 min), and the trachea was connected to a small animal ventilator. A 7-0 suture was used to ligate the LAD coronary artery, and an electrophysiological apparatus (BIOPAC, USA) was connected to measure the electrocardiogram (ECG). Success was considered when the ST-segment elevation $\geq 0.2\text{ mV}$ on ECG and the anterior heart wall became discolored. Meanwhile, the sham group received the same procedures except for ligating LAD coronary artery. After the operation, mice were treated with physiological saline or DAPA. Based on previous studies [15–17], DAPA was dissolved in saline at a concentration of 1 mg/kg and was given daily by gavage.

2.3. Cell culture and treatment

Primary mouse cardiomyocytes (NMCs) were isolated from the ventricles of neonatal C57 mice (aged 1–2 days; Experimental Animal Center, The First Affiliated Hospital of Chongqing Medical University, Chongqing, China). According to the experimental method of previous studies [18]. In simple terms, after anesthetizing mice, the ventricles were removed and cut, the cardiomyocytes were digested with trypsin and collagenase, and the cardiomyocytes were collected after 1000 g centrifugation for 5min, resuspended in Dulbecco's modified Eagle's medium (DMEM)-F-12 (Gibco, Shanghai, China), 10% fetal bovine serum (FBS; HyClone, Logan, UT), penicillin (100 U/mL) and streptomycin (100U/mL); and cultured in an incubator in the condition with 5% CO_2 and 95% air (CON group) at $37\text{ }^{\circ}\text{C}$. DAPA was dissolved in DMSO and used at a concentration of 10 μM based on previous studies [11,13].

To simulate the myocardial infarction, NMCs were placed in a hypoxic chamber with 1% O_2 , 5% CO_2 and 94% N_2 for 24 h (Hy group). The DAPA or Compound C (CC, an AMPK α inhibitor, 10 μM) was given prior to hypoxic treatment (Hy + DAPA group or Hy + DAPA + CC group). After the culture ended, the cells were collected for further identification, and the related protein was analyzed by Western blot.

2.4. Echocardiographic assessment

Echocardiography was performed to evaluate cardiac function in mice. After four weeks of treatment, the mice were anesthetized by inhalation of 2% isoflurane, and L8-18i-D PROBE ultrasound probe (GE Healthcare, Boston, MA, USA) was positioned at the level of papillary muscle to obtain the M-mode images. The following variables were measured and averaged from two consecutive cardiac cycles: left ventricular internal systolic dimension (LVIDs), and left ventricular internal diastolic dimension (LVIDd). Left ventricular

ejection fraction (LVEF) and left ventricular fractional shortening (LVFS) values were converted by Simpson's method. Ultrasound measurements were performed by investigators unaware of the experiment.

2.5. MDA and GSH-PX assay *in vivo/vitro*

In vivo, at the end of the 4-week treatment, all mice were fasted for 12 h and then anesthetized by inhalation of 2% isoflurane. The blood samples were taken through the orbital vein and the supernatant was separated after centrifugation at 12,000 g for 15 min and collected for further analysis. *In vitro*, cells were lysed using RIPA Lysis Buffer. After centrifugation at 12,000 g for 15min, supernatants were collected for further analysis. The concentrations of Malondialdehyde (MDA) and Glutathione Peroxidase (GSH-PX) were measured by MDA assay kit and GSH-PX assay kit according to the manufacturer's instructions (Nanjing Jiancheng Bioengineering Institute, Nanjing, China). Thibabaturic Acid method was used to measure MDA and GSH-PX activity was detected by a colorimetric method.

2.6. Cardiac morphological examination

Mice were anesthetized by inhalation of 2% isoflurane, ribs were cut open, the hearts were excised and the tibia of the left hind limb was removed. Calculate the ratio between the diameter of the long axis of the heart and the length of the tibia of the left hind limb. Subsequently, the heart was fixed by immersion in 4% paraformaldehyde, then dehydrated in an ethanol gradient, embedded in paraffin, and transected along the short axis of the heart into 5 μ m thick sections. Dewax the sections with xylene and alcohol, and stain them with hematoxylin and eosin for morphological observation. At the same time, Masson's trichrome staining was used to assess the extent of fibrosis in cardiac muscle following the instruction steps. ImageJ software was used to quantify the positive staining rate in each sample.

2.7. Cardiac immunohistochemical analysis

To observe the expression of cardiac oxidative stress and apoptosis related proteins, the tissue slides were dewaxed, rehydrated and washed. For antigen retrieval, the sections were immersed in 3% hydrogen peroxide for 10min and blocked of unspecific binding by 5% BSA and incubated with primary antibodies against iNOS (1:50, ab283655, Abcam), p-AMPK α (1:100, AF3423, Affinity) and Cleaved caspase-3 (1:100, AF7022, Affinity) overnight at 4 °C. Thereafter, the slides were incubated with HRP-labeled Goat Anti-Rabbit IgG at 37 °C for 30 min and washed in PBS three times followed by DAB staining. Finally, myocardial structures were visualized under a Leica DM4B microscope. ImageJ software was used to quantify the mean fluorescence in each sample.

2.8. Reactive oxygen species detection *in vivo/vitro*

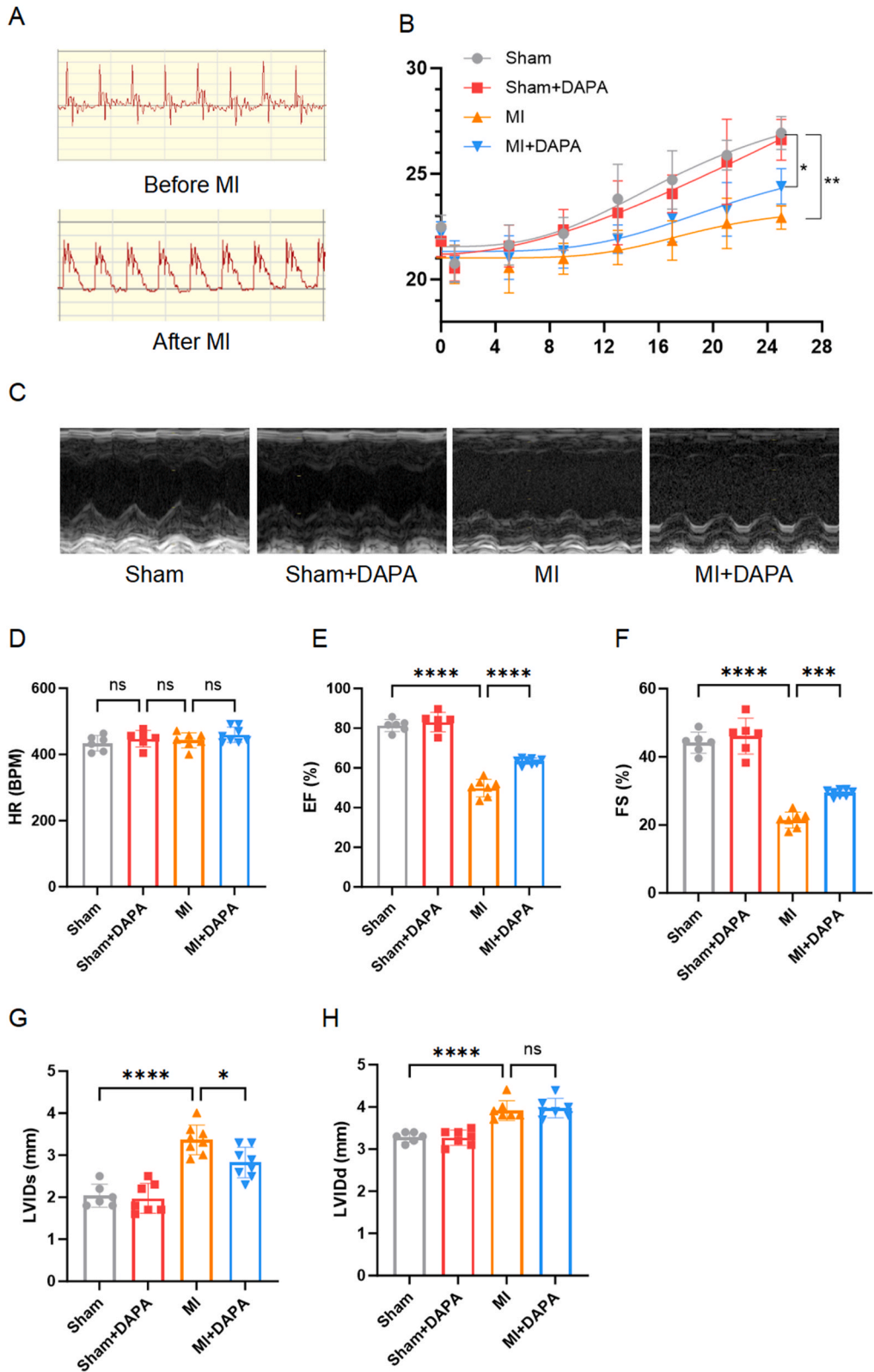
Dihydroethidium (DHE) stains DNA with red fluorescence by specifically reacting with superoxide to form ethidium. *In vivo*, heart tissues were embedded in liquid nitrogen and sectioned into 5- μ m thick slices. The frozen slides were then allowed to thaw at room temperature and incubated with a spontaneous fluorescence quenching reagent for 5 min. Subsequently, the slides were incubated with a ROS staining solution for 30 min in a dark environment at 37 °C and washed with PBS three times. Following this, the slides were incubated with DAPI solution at room temperature for 10 min in the dark and observed using fluorescence microscopy to examine ethidium fluorescence (which emits red light at an excitation wavelength 510–560 nm and an emission wavelength of 590 nm). *In vitro*, cells were incubated with DCFH-DA (10 μ m) for 30 min in a dark environment and then washed with serum-free medium three times to remove any residual DCFH-DA. Fluorescence intensity images were captured using fluorescence microscopy (DCFH-DA is excited at 488 nm, and its emission occur at 525 nm). ImageJ software was employed to quantify the mean fluorescence in each sample. Five different regions were randomly selected for analysis.

2.9. TUNEL assay *in vivo/vitro*

In vivo, after deparaffinized with xylene, the heart slides were incubated with proteinase K solution (20 μ g/ml) for 30 min at room temperature and rinsed three times with PBS. *In vitro*, cells were fixed with immunostaining fixative and incubated with enhanced immunostaining permeabilization buffer for 5 min at room temperature. Then, slides or cells were incubated with TdT-mediated dUTP Nick-End Labeling (TUNEL) reaction mixture for 60 min at 37 °C in a humidified chamber in the dark. Then, washed with PBS for three times, slides or cells were incubated with DAPI for 10 min at room temperature. The TUNEL positive cells were stained with green fluorescence while the DAPI positive cells were stained with blue fluorescence. The levels of apoptosis were calculated as a percentage of the number of TUNEL positive cells over the total number of DAPI positive cells. Five different regions were randomly selected for each sample for analysis.

2.10. Western blot analysis

Cells or tissues were lysed in Radio Immunoprecipitation Assay (RIPA) lysis buffer for 1 h at 4 °C and then centrifuged at 12,000 \times g for 15min. The protein supernatant was concentrated and measured with a BCA protein assay kit. Subsequently, the proper amount of protein sample was separated by sodium dodecyl sulfate polyacrylamide gel electrophoresis (SDS-PAGE). Then, the gel with the



(caption on next page)

Fig. 1. Dapagliflozin improved cardiac function in MI mice. At the time of infarction surgery, mice were tested for ECG and ST-segment elevation indicated successful surgery. After the infarction surgery, DAPA (1 mg/kg) was given daily by gavage for four weeks. The body weight of the mice was recorded at 4-day intervals and the cardiac function of mice was measured after four weeks. (A) Electrocardiograms before and after infarction surgery. ST-segment elevation is evidence of successful infarction surgery (n = 6). (B) Changes in body weight of mice before and after surgery (n = 6). Comparisons were performed using one-way ANOVA for multiple groups. (C) Typical images of left ventricular M-mode echocardiograms of mice in different experimental groups. (D) Statistical analysis of heart rate (n = 6). Comparisons were performed using one-way ANOVA for multiple groups. (E) LVEF's statistical analysis (n = 6). Comparisons were performed using one-way ANOVA for multiple groups. (F) Statistical analysis of LVFS (n = 6). Comparisons were performed using one-way ANOVA for multiple groups. (G) LVIDs's statistical analysis (n = 6). Comparisons were performed using one-way ANOVA for multiple groups. (H) Statistical analysis of LVIDd (n = 6). Comparisons were performed using one-way ANOVA for multiple groups. Data are presented as the mean \pm SEM. *p < 0.05, **p < 0.01, ***p < 0.001, ****p < 0.0001, N.S. not significant.

protein was cut horizontally according to the corresponding molecular weight and transferred to polyvinylidene fluoride (PVDF) membranes. Blocked with 5% milk, the membranes were incubated overnight at 4 °C with primary antibodies: p-AMPK α (1:1000, A5740, Bimake), AMPK α (1:1000, A5008, Bimake), Nrf2 (1:1000, BF8017, Affinity), NOX4 (1:4000, 14347-1-AP, Proteintech), NOX2 (1:2000, 19013-1-AP, Proteintech), NQO1 (1:1000, A5464, Bimake), SOD2 (1:10000, 24127-1-AP, Proteintech), Cleaved caspase-3 (1:1000, 29034, Signalway Antibody), Bax (1:2000, 50599-2-Ig, Proteintech), Bcl-2 (1:1000, 26593-1-AP, Proteintech) and β -Actin (1:5000, 20536-1-AP, Proteintech). Membranes were incubated with horseradish peroxidase conjugated secondary anti-rabbit or anti-mouse IgG (1:10000, ThermoFisher Scientific, USA) for 1 h at room temperature. Finally, Proteins were detected with a chemiluminescence reagent kit (Biosharp, Beijing, China), and the protein concentration was quantified by Quantity One Software (BioRad).

2.11. Statistical analysis

Numeric values were all expressed as the means \pm standard deviation (SD) and Shapiro-Wilk normality test was used to assess the normality of the distribution of data. Normally distributed data were analyzed by unpaired 2-tailed Student's t-tests between two groups. The comparisons of multiple groups (≥ 6 groups) were made by one-way analysis of variance (ANOVA) followed by Scheffe's test, Bonferroni post hoc test or Dunnett's multiple-to-one comparison test. Data analysis and graphing were performed using GraphPad Prism 9.0, and a p-value < 0.05 was considered statistically significant.

3. Results

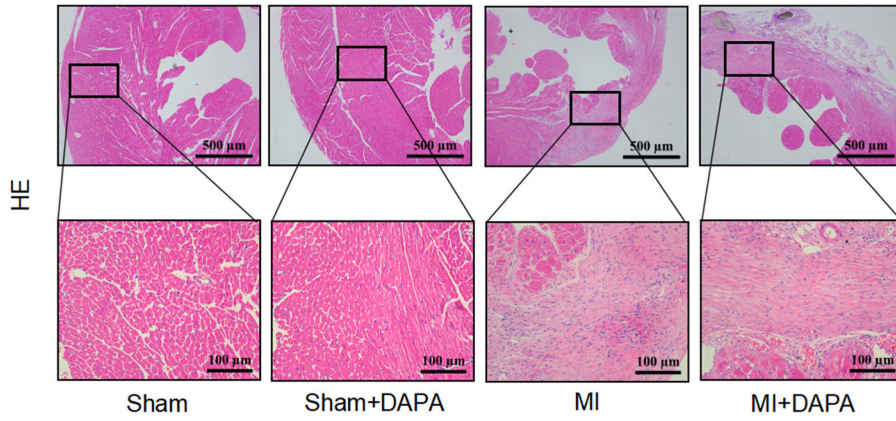
3.1. Dapagliflozin improved cardiac function in MI mice

At the end of the mouse ligation of the LAD, an electrocardiogram was used to check whether the operation was successful. As shown in Fig. 1A, the ECG ST-segment elevation confirms the model's success. Clinical studies have shown that weight loss after MI is associated with worse prognosis [19]. Therefore, we monitored weight changes after MI, as shown in Fig. 1B, the body weight of the MI group was generally lower than that of the Sham group and Sham + DAPA group, while this change was reversed in the treatment group, suggesting that the DAPA treatment can increase the body weight of MI group. In our daily observation, the mice showed reduced exercise and eating, and slow weight gain after MI, and DAPA treatment improved these symptoms. This may represent a favorable prognosis for MI mice. To investigate the effect of DAPA on cardiac function in mice with myocardial infarction, we used echocardiography to evaluate the cardiac function of each group of mice after four weeks of MI surgical treatment. Representative echocardiographic images were shown in Fig. 1C. The results showed that MI led to a significant decrease in LVEF and LVFS, and the DAPA treatment reversed this change, indicating that DAPA could restore the cardiac function of MI mice (Fig. 1D–F). Subsequently, we examined LVIDs and LVIDd in mice, and we found that DAPA improved cardiac function mainly by reducing LVIDs (Fig. 1G–H).

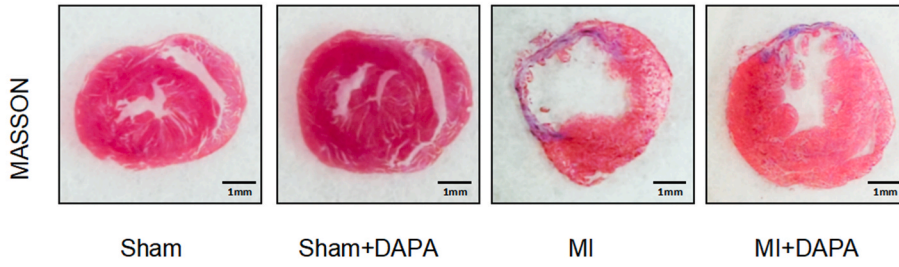
3.2. Dapagliflozin alleviated ventricular remodeling

Subsequently, we used HE staining to assess the degree of myocardial injury in mice. Compared with the Sham group, HE staining of MI showed increased myocardial cell inflammatory infiltration. In the MI group, the cells were swollen and ruptured, and a large number of inflammatory cells were infiltrated. DAPA treatment alleviated the inflammatory response and reduced cell deformation (Fig. 2A). Masson staining was used to detect the degree of myocardial fibrosis in mice (Fig. 2B). The statistics showed that the left ventricle of mice had obvious fibrosis after myocardial infarction, and DAPA treatment could significantly improve the fibrosis in myocardial infarction mice (Fig. 2C). Therefore, we further measured the size of the long axis of the heart. After MI, ventricular remodeling occurs, and fibrosis often leads to increased heart length, and DAPA treatment attenuated ventricular remodeling in mice (Fig. 2D–E). In conclusion, morphological results demonstrated that DAPA could improve impaired cardiac function and mitigate adverse cardiac remodeling in mice with myocardial infarction. MDA (an indicator of lipid peroxidation) and GSH-Px (antioxidant enzymes active against free radicals) are oxidative stress markers. To determine the level of oxidative stress, we detected the levels of MDA and GSH-PX in mouse serum, As shown in Fig. 2F and G, GSH-PX activity decreased and MDA content increased in MI group mice, indicating that MI-induced oxidative stress in the heart. MI-induced oxidative stress was inhibited by DAPA by restoring GSH-PX activity and reducing MDA level. Subsequently, we examined the expression of SGLT2 in the hearts and kidneys of mice, as shown in Fig. 2H. SGLT2 is highly expressed in the kidneys, but hardly expressed in the heart, which is consistent with previous studies [20].

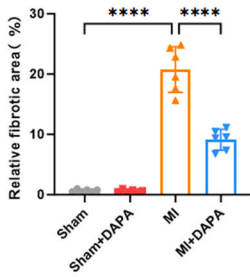
A



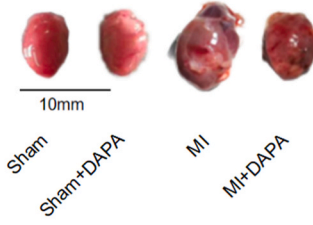
B



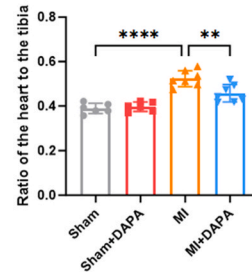
C



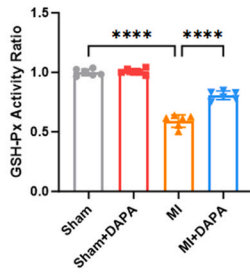
D



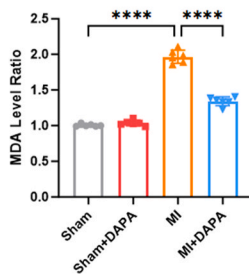
E



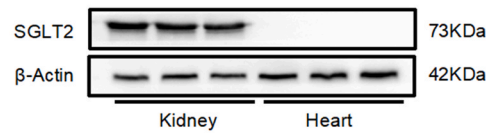
F



G



H



(caption on next page)

Fig. 2. Dapagliflozin alleviated ventricular remodeling post MI *in vivo*. (A) HE staining. Sham group and Sham + DAPA group showed regularly arranged cardiomyocytes with intact nuclei. The MI group showed distorted nuclei, swollen and ruptured cells, and a large number of inflammatory cells infiltrated, while the MI + DAPA group showed a relatively regular arrangement of cells and reduced infiltration of inflammatory cells (n = 6). (B) Masson staining of tissue. (C) Statistical analysis of the myocardial fibrotic area. Fibrotic area (%) = fibrillated region/LV area *100% (n = 6). Comparisons were performed using one-way ANOVA for multiple groups. (D) The size of the long axis of the heart. (E) The ratio of the heart to the tibia. The calculation method was the ratio between the diameter of the long axis of the heart and the length of the tibia of the left hind limb (n = 6). Comparisons were performed using one-way ANOVA for multiple groups. (F) GSH-PX activity and MDA content in mice serum were measured using related kits. Statistical analysis of serum GSH-PX activity ratio (n = 6). Comparisons were performed using one-way ANOVA for multiple groups. (G) Statistical analysis of serum MDA level ratio (n = 6). Comparisons were performed using one-way ANOVA for multiple groups. (H) Relative expression of SGLT2 protein in the heart and kidney (n = 6). **p < 0.01, ***p < 0.001, ****p < 0.0001.

3.3. Dapagliflozin attenuated cardiomyocyte oxidative stress *in vivo*

DAPA can reduce the level of serum oxidative stress, which means that it may reduce myocardial oxidative stress injury. Therefore, we further explored its effect on the myocardium. The NRF2 and NQO1 proteins play a crucial role as antioxidants, and the NRF2/NQO1 pathway serves as a vital signaling mechanism regulating oxidative stress. NADPH oxidase (NOX) 2 and 4 are key enzymes involved in electron transfer in cell membranes and contribute to oxidative stress under pathological environments [21–23]. Western blot analysis showed that DAPA, on the one hand, reduced ROS production by decreasing NOX2 and NOX4. On the other hand, DAPA treatment significantly enhanced SOD activity and increased the expression of NRF2 and NQO1 (Fig. 3A and B). Inducible Nitric Oxide Synthase (iNOS) can continuously accumulate superoxide and increase the level of oxidative stress [24,25], so we detected the expression of iNOS in the myocardial tissue of mice by immunohistochemistry (Fig. 3C and D). The expression of iNOS in the myocardial tissue in MI group was significantly higher than the Sham group, which was decreased after DAPA treatment, indicating that DAPA treatment can reduce the level of oxidative stress caused by myocardial infarction. DHE staining further confirmed this conclusion. DHE was used to evaluate the superoxide anion in the left ventricular tissue of mice. The results showed that compared with the MI group, the myocardial superoxide anion content of the MI + DAPA group was significantly decreased (Fig. 3E and F). In a word, these results suggested that DAPA reduces myocardial oxidative stress levels in mice with MI.

3.4. Dapagliflozin prevented cardiac apoptosis *in vivo*

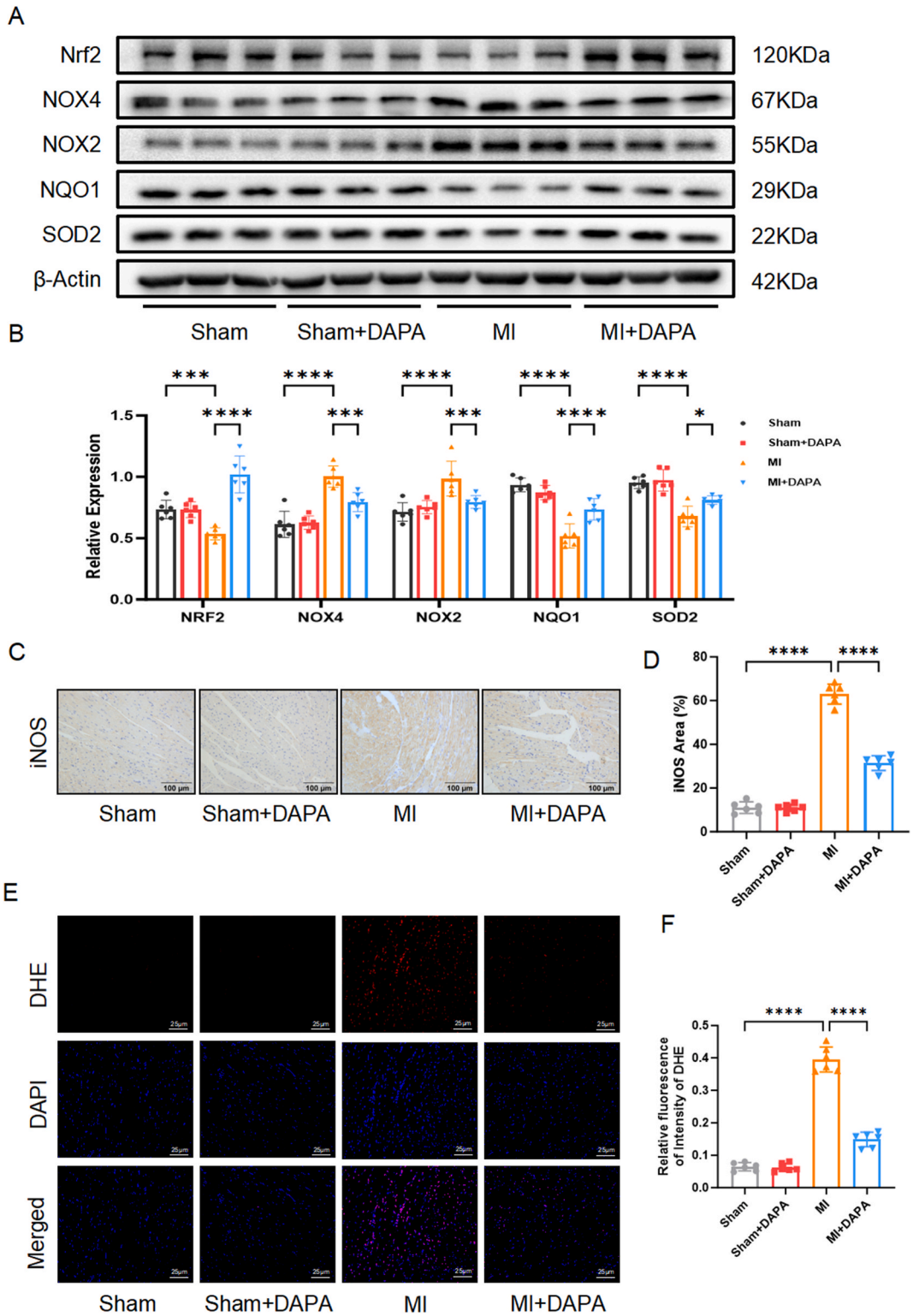
ROS and the resulting oxidative stress play a key role in apoptosis, and excess stress kills cells either by apoptosis or apoptosis [26]. Cells use antioxidant defense mechanisms to counteract the damaging effects of ROS. Apoptosis can prevent cells from losing control in the face of persistent oxidative stress. Previous studies have shown that Bcl-2 can enhance the endogenous antioxidant capacity of cells and prevent cells from entering the process of apoptosis [27,28]. Our previous study has demonstrated that DAPA can alleviate oxidative stress, so we decided to further examine its effect on apoptosis. We analyzed the expression of apoptosis-related proteins BAX and Bcl-2 in myocardial tissue by Western blot. Compared with the Sham group, the expression of Bcl-2 in the MI group was significantly decreased, while the ratio of BAX/Bcl-2 was increased. Dapagliflozin treatment significantly reduced the values of BAX and up-regulated Bcl-2 expression (Fig. 4A and B). Then, we analyzed the expression of Cleaved caspase-3 by immunohistochemistry (Fig. 4C and D). The MI group showed increased Cleaved caspase-3 content in cardiomyocytes. In contrast, the MI + DAPA group showed moderate expression of Cleaved caspase-3, indicating that DAPA alleviates myocardial cell apoptosis. Finally, apoptosis was assessed by TUNEL staining. As shown in Fig. 4E and F, the proportion of TUNEL-positive cardiomyocytes was significantly reduced after DAPA treatment compared with the MI group. MI increased the expression of apoptotic proteins to induce apoptosis, while DAPA treatment significantly reversed all these variations. These results indicate that DAPA can significantly reduce the level of cardiomyocyte apoptosis after MI.

3.5. Dapagliflozin activated AMPK α phosphorylation *in vivo/vitro*

Previous studies have suggested that AMPK α can activate NRF2 to exert an antioxidant cascade [29]. To explore whether DAPA exerts its antioxidant effect by activating AMPK α , we examined the expression in the MI group and DAPA treatment group. Western Blot results showed that MI treatment decreased phosphorylated AMPK α in MI mice, and DAPA treatment restored this change (Fig. 5A and B). Immunofluorescence of myocardial tissue confirmed our results (Fig. 5C and D). Subsequently, we verified this result in NCMCs cells, where hypoxia resulted in the inhibition of AMPK α phosphorylation (Fig. 5C and D), and DAPA treatment significantly restored the phosphorylation of AMPK α (Fig. 5E and F). These results suggest that DAPA may play a protective role in MI heart by activating the AMPK α signaling pathway.

3.6. Dapagliflozin plays a protective role by promoting AMPK α phosphorylation *in vitro*

We found that DAPA activates AMPK α phosphorylate. To investigate whether the protective effect of DAPA was dependent on the activation of AMPK α , we treated NCMCs with hypoxia and CC, and observed the changes in apoptosis and oxidative stress indicators. Firstly, we measured the contents of GSH-PX and MDA in the cells. Hypoxia led to the increase of MDA level in the cells, and although DAPA decreased MDA level in the cells, CC reversed the protective effect (Fig. 6A and B). Then, the results of Western Blot showed that NOX4 content and BAX/Bcl-2 ratio increased, NRF2, NQO1 and SOD2 expression decreased, and P-AMPK α expression was inhibited



(caption on next page)

Fig. 3. Dapagliflozin attenuated cardiomyocyte oxidative stress *in vivo*. (A) Target proteins were examined by Western blotting. Representative protein blotting results are shown in figure. (B) Statistical analysis of NRF2/ β -Actin, NOX4/ β -Actin, NOX2/ β -Actin, NQO1/ β -Actin, SOD2/ β -Actin (n = 6). Comparisons were performed using one-way ANOVA for multiple groups. (C) The expression and location of iNOS were determined by immunohistochemistry. (D) Statistical analysis of iNOS area (n = 6). Comparisons were performed using one-way ANOVA for multiple groups. (E) The expression and location of ROS were determined by immunofluorescence. (F) Statistical analysis of fluorescence intensity (n = 6). Data are presented as the mean \pm SEM. Comparisons were performed using one-way ANOVA for multiple groups or Student's t-test for two groups. *p < 0.05, **p < 0.01, ***p < 0.001, ****p < 0.0001.

after hypoxia treatment. However, this protein expression of the DAPA treatment group recovered, suggesting that DAPA could attenuate oxidative stress injury and apoptosis of cells *in vitro*. Subsequently, CC was added to Hy + DAPA cells, and as shown in Fig. 6C, CC blocked the expression of P-AMPK and abolished the inhibitory effect of DAPA on NOX4 expression and BAX/Bcl-2 ratio. In addition, CC attenuated the enhanced expression of antioxidant proteins Nrf2, SOD2 and NQO1 induced by DAPA. Meanwhile, the detection of ROS by fluorescence staining showed that DAPA could reduce ROS in hypoxia-injured NCMs, while CC eliminated the protective effect of DAPA on cells (Fig. 6E).

In conclusion, our study found that DAPA mediated AMPK α phosphorylation, but after CC inhibited AMPK α phosphorylation, the protective effect of DAPA on oxidative stress and cell apoptosis was weakened, indicating that AMPK α plays a crucial role in DAPA treatment. DAPA activates NRF2/NQO1 and inhibits Bax/Bcl-2 phosphorylation dependent on AMPK α .

4. Discussion

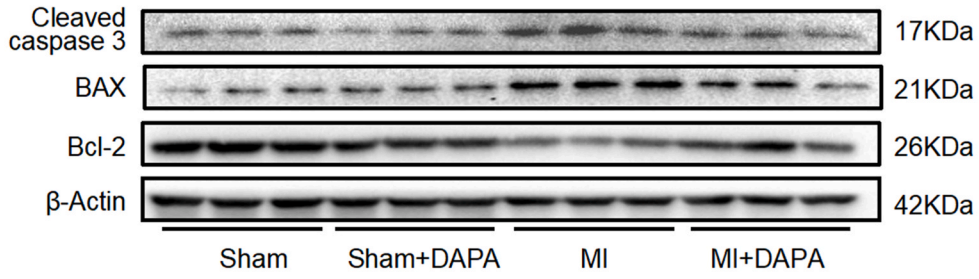
This study reveals two novel findings regarding the protective effects of DAPA on the myocardium. Firstly, we demonstrate that DAPA effectively mitigates ventricular remodeling resulting from myocardial infarction, suggesting that it may safeguard the heart by minimizing the damage caused by such infarctions. Secondly, we demonstrated that its protective effect is related to the activation of AMPK α , and that DAPA reduces oxidative stress and apoptosis by activating AMPK α . Consequently, our findings shed light on potential mechanisms of DAPA's cardiac protection, positioning it as a promising novel treatment for myocardial infarction.

Since FDA approval, SGLT2 inhibitors have been widely used for the treatment of patients with type 2 diabetes combined with cardiovascular disease. Previous studies have shown that since SGLT2 is not generated and expressed in cardiomyocytes [30,31], the cardioprotective effect of SGLT2 inhibitions in patients with diabetic heart failure is through attenuating cardiac load by reducing renal reabsorption, reducing hyperglycemia and lowering the diuretic sodium. In recent years, several studies have pointed out that SGLT2 inhibitors exhibit cardioprotective effects independent of their antihyperglycemic properties. Carlos et al. reported that SGLT2 inhibitors empagliflozin ameliorate adverse heart failure and cardiac remodeling in a non-diabetic pig model [32]. Anker et al. found that SGLT2 could reduce the risk of cardiac death and improve heart failure in patients without diabetes and exert a cardioprotective effect in patients without diabetes [33]. However, the exact mechanism has not been fully elucidated. Myocardial infarction causes cardiac dysfunction and adverse ventricular remodeling, which can easily trigger sudden cardiac death and lead to high mortality. In this experiment, we evaluated the effect of DAPA, an SGLT2 inhibitor, on MI in non-diabetic mice. Consistent with previous studies in diabetic mice, we found that DAPA treatment restored ventricular remodeling and improved cardiac function and ejection fraction after MI. In addition, we found that LVIDs in mice were restored after DAPA treatment, while LVIDd was barely changed, implying that DAPA may exert protective effects mainly by affecting LVIDs. We measured body weight changes in mice after MI, and we found that MI caused weight loss in mice, whereas DAPA treatment restored body weight in mice after MI, and clinical studies pointed out that weight loss after MI was associated with worse prognosis. This suggests that DAPA may directly affect the heart and exert a protective effect after MI rather than through glucose and water sodium regulation.

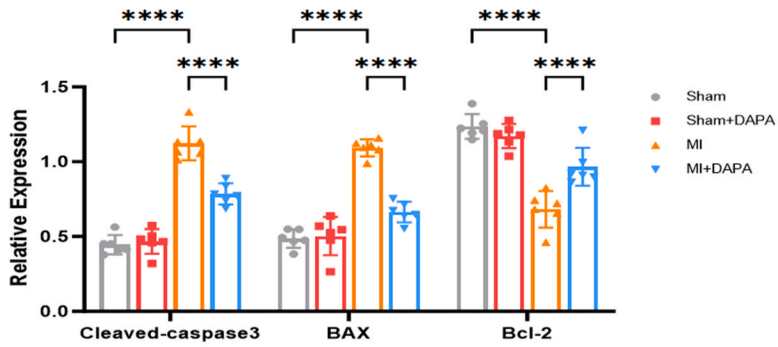
After MI, cells will undergo oxidative stress, and NADPH oxidase has been proven to be an essential source of ROS in myocardial tissue [34–36]. Under pathological conditions, it generates excessive ROS, which exceeds the antioxidant capacity of cells, leads to protein and DNA damage and promotes the development of cardiomyocyte fibrosis and apoptosis. NRF2 is an oxidative stress-induced transcription factor that plays a protective role by inducing the transcription of genes containing antioxidant response elements and activating enzymes and proteins that prevent lipid peroxidation [37–39]. Previous studies have reported that SGLT inhibitor treatment significantly improves myocardial oxidative stress in type II diabetic rats [40]. However, its cardioprotective mechanism in non-diabetic mice deserves further investigation. In the myocardium of MI mice, we detected a significant increase in MDA, decreased GSH-Px activity, accumulation of NOX2 and NOX4, and downregulation of the NRF2/NQO1 antioxidant pathway. These results indicate that severe oxidative stress injury occurs in the myocardium after MI. DAPA treatment significantly reduced MDA levels and restored GSH-Px activity in the myocardial tissue of MI mice. It also activated the NRF2/NQO1 pathway and inhibited NOX2/NOX4 to improve oxidative stress, which is consistent with previous studies [17]. These findings suggest that the protective effect of DAPA on the heart may be generated through the inhibition of oxidative stress.

Apoptosis is another mechanism of cell injury. Myocardial infarction leads to increased inflammatory responses in cardiomyocytes and up-regulation of the apoptotic marker caspase-3, which eventually leads to apoptosis of cardiomyocytes [41,42]. Previous studies have found that DAPA may attenuate the progression of cardiac dysfunction by reducing inflammasome activation and attenuating apoptosis [43], and in the myocardial tissue of diabetic mice, DAPA can play a protective role by reducing apoptosis [44]. In the present study, we found a significant increase in BAX/Bcl-2 in the myocardial tissue of MI mice, suggesting that apoptosis is involved in the development of MI. However, DAPA treatment significantly reduced the expression of caspase-3 and the ratio of BAX/Bcl-2, and attenuated myocardial apoptosis after myocardial infarction. Therefore, our study suggests that inhibition of cardiomyocyte apoptosis may be a mechanism by which DAPA exerts cardioprotective effects.

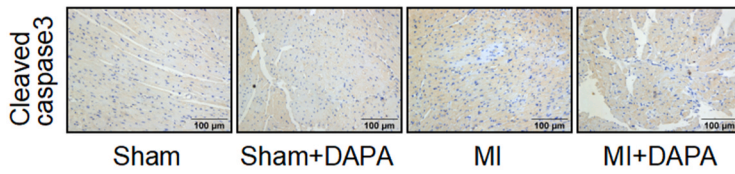
A



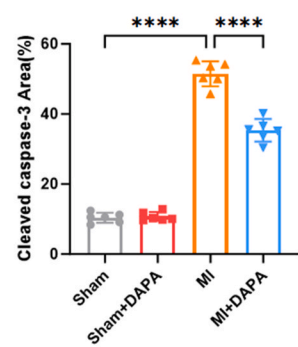
B



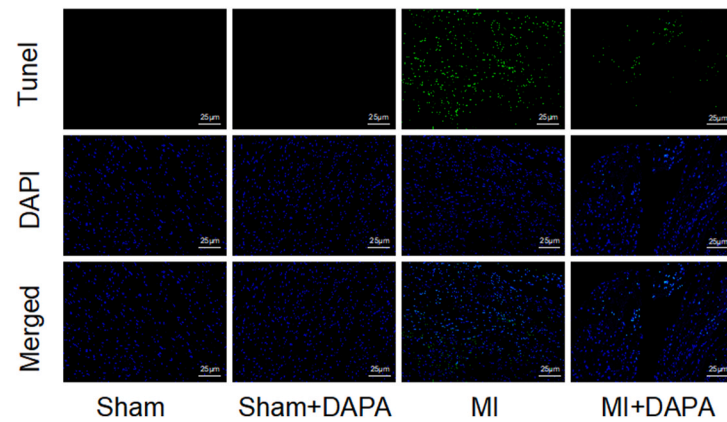
C



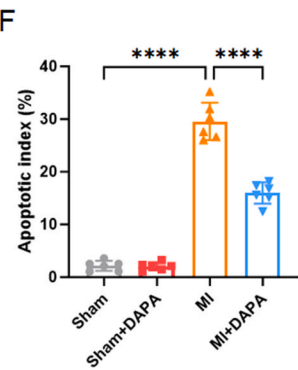
D



E



F



(caption on next page)

Fig. 4. Dapagliflozin prevented cardiac apoptosis *in vivo*. (A) Total heart proteins were extracted and the expression of Cleaved-caspase3, BAX and Bcl-2 was detected by western blotting. Representative protein blotting results are shown in figure. (B) Statistical analysis of Cleaved-caspase3/ β -Actin, BAX/ β -Actin, Bcl-2/ β -Actin (n = 6). Comparisons were performed using one-way ANOVA for multiple groups. (C) The expression and location of Cleaved-caspase3 were determined by immunohistochemistry. (D) Statistical analysis of Cleaved-caspase3 area (n = 6). Comparisons were performed using one-way ANOVA for multiple groups. (E) Cardiac tissues were detected using TUNEL staining. Representative images of TUNEL assay. Apoptotic cardiomyocytes were labeled using TUNEL staining, and DAPI was used to detect nuclei. (F) Apoptotic index's statistical analysis. Apoptotic index = TUNEL-positive cells/DAPI-positive cells \times 100% (n = 6). Data are presented as the mean \pm SEM. Statistical analysis was performed using 2-way ANOVA with a Tukey's multiple-comparison post-hoc test comparisons between multiple groups. *p < 0.05, **p < 0.01, ***p < 0.001, ****p < 0.0001.

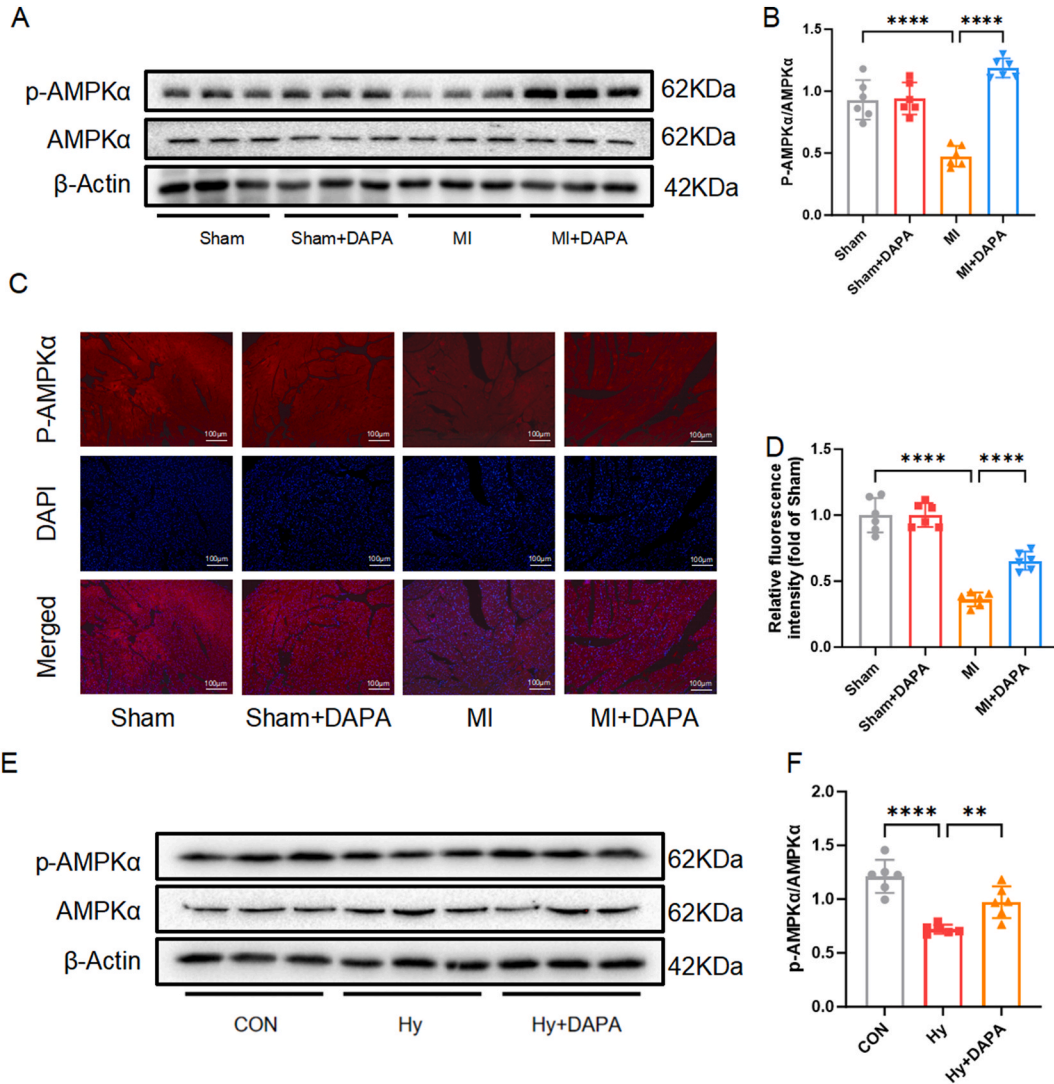
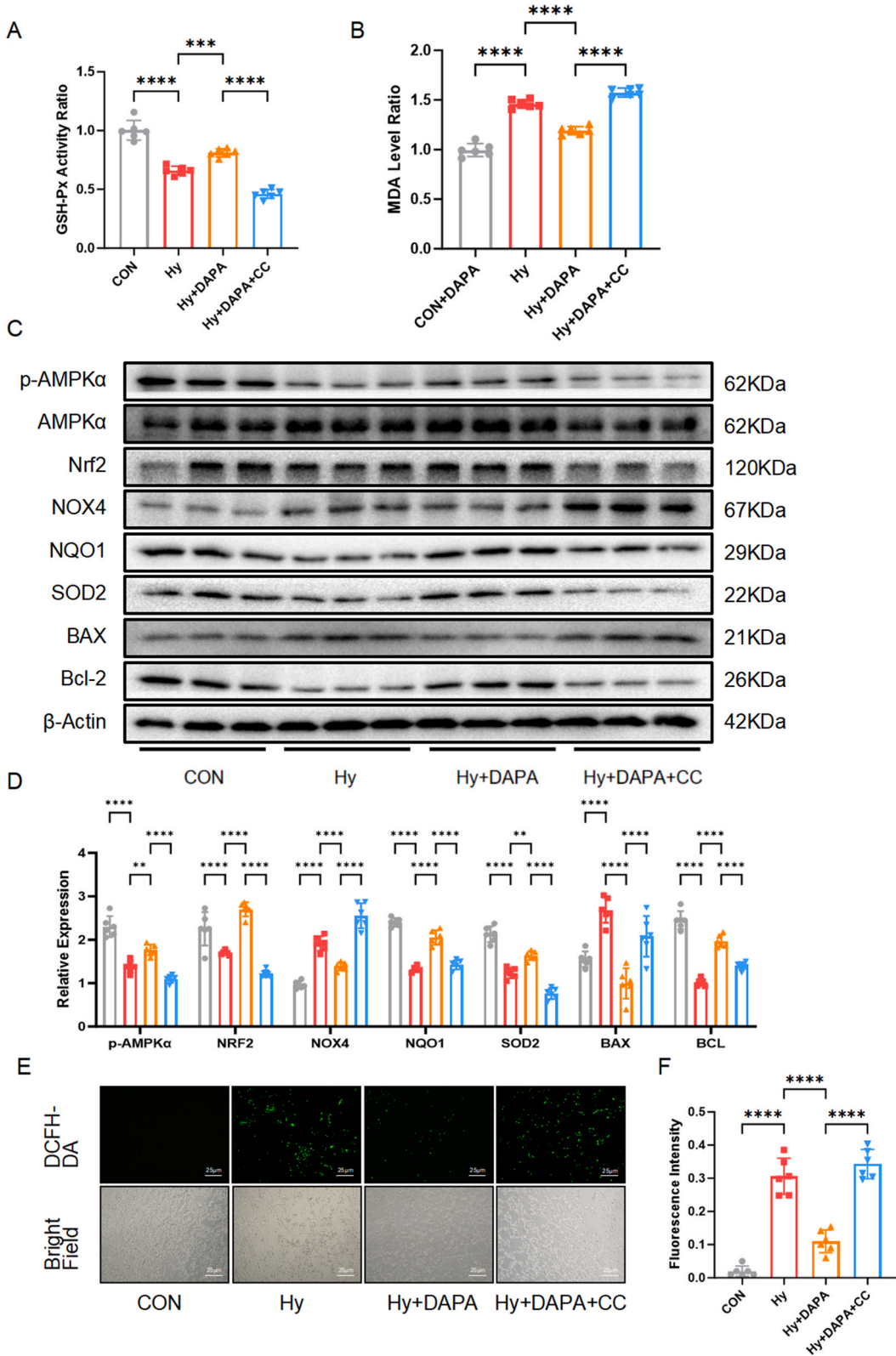


Fig. 5. Dapagliflozin activated AMPK α phosphorylation *in vivo/vitro*. (A) Total proteins were extracted and the expression of p-AMPK α and AMPK α was detected by western blotting in myocardial tissue. Representative protein blotting results are shown in figure. (B) Statistical analysis of p-AMPK α /AMPK α (n = 6). Comparisons were performed using one-way ANOVA for multiple groups. (C) The expression and location of p-AMPK α were determined by immunofluorescence. (D) Statistical analysis of p-AMPK α relative fluorescence intensity (n = 6). Data are expressed as means \pm SD, comparisons were performed using one-way ANOVA for multiple groups. (E) Total proteins were extracted and the expression of p-AMPK α , AMPK α was detected by western blotting in NMCs. Representative protein blotting results are shown in figure. (F) Statistical analysis of p-AMPK α /AMPK α (n = 6). Data are presented as the mean \pm SEM. Statistical analysis was performed using 2-way ANOVA with a Tukey's multiple-comparison post-hoc test comparisons between multiple groups. *p < 0.05, **p < 0.01, ***p < 0.001, ****p < 0.0001.



(caption on next page)

Fig. 6. Dapagliflozin plays a protective role by promoting AMPK α phosphorylation *in vitro*. (A) GSH-PX activity and MDA content in cell lysis solution were measured using related kits. Statistical analysis of serum GSH-PX activity ratio (n = 6). Comparisons were performed using one-way ANOVA for multiple groups. (B) Statistical analysis of serum MDA level ratio (n = 6). Comparisons were performed using one-way ANOVA for multiple groups. (C) Target proteins were examined by western blotting. Representative protein blotting results are shown in figure. (D) Statistical analysis of p-AMPK α /AMPK α , NRF2/ β -Actin, NOX4/ β -Actin, NQO1/ β -Actin, SOD2/ β -Actin, BAX/ β -Actin, Bcl-2/ β -Actin (n = 6). Comparisons were performed using one-way ANOVA for multiple groups. (E) The expression of ROS was determined by immunofluorescence. (F) Statistical analysis of fluorescence intensity (n = 6). Data are presented as the mean \pm SEM. Statistical analysis was performed using 2-way ANOVA with a Tukey's multiple-comparison post-hoc test comparisons between multiple groups. *p < 0.05, **p < 0.01, ***p < 0.001, ****p < 0.0001.

AMPK α plays an important role in the regulation of glucose homeostasis and whole-body energy metabolism. Studies have found that inhibition of AMPK α phosphorylation can lead to a decrease in the survival rate of cardiomyocytes, and the activation of AMPK α may be one of the potential mechanisms of its cardioprotective effect [45]. A new study points out that AMPK acts upstream of NRF2 and induces NRF2 upregulation through phosphorylation [46]. Consistent with the above studies, we found synchronous changes in NRF2/NQO1 signaling after alteration of AMPK α activity, indicating that DAPA activation of NRF2/NQO1 is dependent on AMPK α phosphorylation. We confirmed this finding by *in vitro* cell culture assays, establishing that the anti-oxidative stress effect of DAPA is associated with AMPK α activation. Hypoxia-induced increased expression of oxidative stress-related proteins in primary cardiac cells. DAPA treatment activated AMPK α and alleviated oxidative stress injury. After treatment with compound C, an inhibitor of AMPK α phosphorylation, NOX was re-increased, suggesting that DAPA may exert its anti-oxidative stress effect in an AMPK α -dependent manner. In addition, it has been shown that AMPK activation can up-regulate Bcl-2 transcription by down-regulating the expression of pro-apoptotic BAX and inhibiting the activation of Caspase3, thereby inhibiting the occurrence of apoptosis [47]. Activation of AMPK α appears to be the key component mediating the anti-apoptotic effect of DAPA. The anti-apoptotic effect of DAPA was abolished when we used the AMPK inhibitor compound C, confirming that DAPA attenuates post-MI injury by activating AMPK α and reducing apoptosis.

Several limitations in this study warrant acknowledgment. Firstly, DAPA, administered orally, may exert effects on the liver and kidneys when treating nondiabetic mice. These effects must be carefully considered in the context of DAPA's use for myocardial infarction treatment, as they could potentially impact its applicability. Secondly, we collected heart tissue four weeks after MI surgery for further analysis, which restricted our exploration of DAPA's effects during the early stages of MI. Notably, the pronounced activation of apoptosis typically occurs one to two weeks after MI, making it more meaningful to investigate DAPA's mechanisms of action within this timeframe. Additionally, the relatively small sample size in each group resulted from rat fatalities due to pneumothorax, intraoperative bleeding, or postoperative cardiac rupture following MI surgery. These limitations may have hindered our comprehensive understanding of DAPA's therapeutic mechanisms. Lastly, while the oxidative stress and apoptosis signaling pathways play pivotal roles in DAPA treatment, further research is needed to elucidate how DAPA impacts antioxidant enzymes and reduces apoptosis in subsequent experiments.

In summary, our study sheds light on the mechanisms underlying the cardioprotective effects of DAPA, as depicted in Fig. 7. We found that DAPA mitigated cardiac remodeling and improved cardiac function in MI mice by inhibiting apoptosis and oxidative stress within the infarcted myocardium. Mechanistically, our *in vitro* experiments revealed that DAPA rescued cardiomyocyte death by

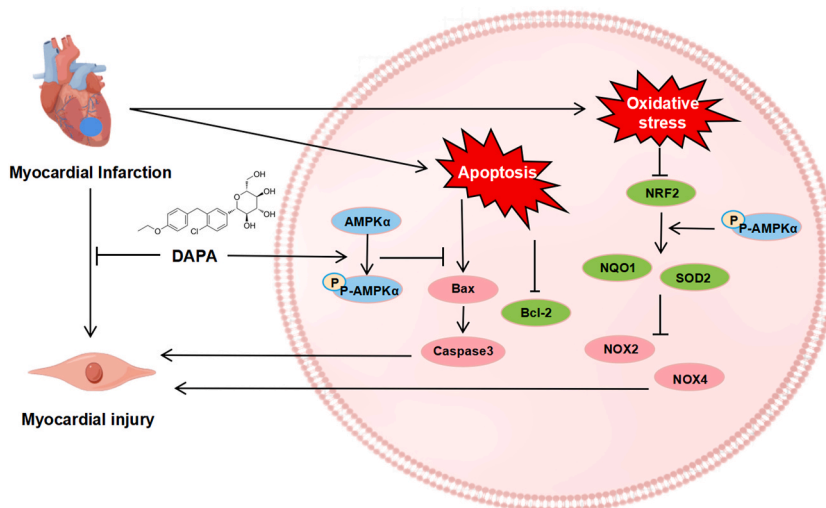


Fig. 7. After myocardial infarction, cardiac myocytes undergo oxidative stress and apoptosis. DAPA, through phosphorylation of AMPK α , activates the expression of antioxidant proteins such as NRF2, NQO1 and SOD2 while inhibiting the expression of the apoptotic marker BAX and Caspase-3. This dual action contributes to antioxidant stress relief and apoptosis attenuation, ultimately reducing ventricular remodeling and improving post-infarction myocardial function.

suppressing oxidative stress and apoptosis in an AMPK α -dependent manner. Consequently, our findings offer fresh insights into potential mechanisms through which DAPA reduces cardiovascular mortality in humans, providing robust evidence for the use of SGLT2 inhibitors. Furthermore, understanding the comprehensive mechanism of DAPA's anti-myocardial infarction effect opens up possibilities for its application in other heart diseases, warranting further exploration.

5. Conclusion

DAPA may play a protective role in MI. Since cardiomyocytes do not express SGLT2, our study demonstrates that DAPA attenuates ventricular remodeling and ameliorates cardiac dysfunction by inhibiting oxidative stress and apoptosis in MI mice. As for the underlying mechanism, *in vitro* studies suggest that DAPA can attenuate oxidative stress and apoptosis induced by MI in an AMPK α -dependent manner, and AMPK α inhibitors can block this effect. Thus, our experiments show the therapeutic promise of DAPA for cardioprotection and provide new insights into its possible mechanisms.

Funding

This work was supported by the National Natural Science Foundation of China (82070238).

Data availability

All data utilized in this study are included in this article, and all data supporting the findings of this study are available on reasonable request from the corresponding author.

CRediT authorship contribution statement

Yuce Peng: Writing – review & editing, Writing – original draft, Visualization, Project administration, Investigation, Formal analysis, Data curation. **Mingyu Guo:** Writing – review & editing, Writing – original draft, Software, Funding acquisition, Conceptualization. **Minghao Luo:** Supervision, Software, Conceptualization. **Dingyi Lv:** Visualization, Methodology, Investigation. **Ke Liao:** Methodology, Formal analysis, Conceptualization. **Suxin Luo:** Visualization, Supervision, Project administration. **Bingyu Zhang:** Writing – review & editing, Visualization, Supervision, Methodology, Investigation.

Declaration of competing interest

The authors declare that they have no known competing financial interests or personal relationships that could have appeared to influence the work reported in this paper.

Appendix A. Supplementary data

Supplementary data to this article can be found online at <https://doi.org/10.1016/j.heliyon.2024.e29160>.

References

- [1] J.C. Kaski, et al., Reappraisal of ischemic heart disease, *Circulation* 138 (14) (2018) 1463–1480.
- [2] M.C. Marc, et al., Pre-revascularization coronary wedge pressure as marker of adverse long-term left ventricular remodelling in patients with acute ST-segment elevation myocardial infarction, *Sci. Rep.* 8 (1) (2018) 1897.
- [3] A. Lewén, P. Matz, P.H. Chan, Free radical pathways in CNS injury, *J. Neurotrauma* 17 (10) (2000) 871–890.
- [4] L.E. Wold, A.F. Ceylan-Isik, J. Ren, Oxidative stress and stress signaling: menace of diabetic cardiomyopathy, *Acta Pharmacol. Sin.* 26 (8) (2005) 908–917.
- [5] H.J. Heerspink, et al., Sodium glucose cotransporter 2 inhibitors in the treatment of diabetes Mellitus: cardiovascular and kidney effects, potential mechanisms, and clinical applications, *Circulation* 134 (10) (2016) 752–772.
- [6] R.E. Kuhre, et al., No direct effect of SGLT2 activity on glucagon secretion, *Diabetologia* 62 (6) (2019) 1011–1023.
- [7] J.J.V. McMurray, et al., Dapagliflozin in patients with heart failure and reduced ejection fraction, *N. Engl. J. Med.* 381 (21) (2019) 1995–2008.
- [8] S.D. Wiviott, et al., Dapagliflozin and cardiovascular outcomes in type 2 diabetes, *N. Engl. J. Med.* 380 (4) (2019) 347–357.
- [9] B. Zinman, et al., Empagliflozin, cardiovascular outcomes, and mortality in type 2 diabetes, *N. Engl. J. Med.* 373 (22) (2015) 2117–2128.
- [10] C. Li, et al., SGLT2 inhibition with empagliflozin attenuates myocardial oxidative stress and fibrosis in diabetic mice heart, *Cardiovasc. Diabetol.* 18 (1) (2019) 15.
- [11] Y.J. Xing, et al., A SGLT2 inhibitor dapagliflozin alleviates diabetic cardiomyopathy by suppressing high glucose-induced oxidative stress in vivo and in vitro, *Front. Pharmacol.* 12 (2021) 708177.
- [12] Z.G. Fan, et al., Appropriate Dose of dapagliflozin improves cardiac outcomes by normalizing mitochondrial fission and reducing cardiomyocyte apoptosis after acute myocardial infarction, *Drug Des. Dev. Ther.* 16 (2022) 2017–2030.
- [13] S. Han, et al., Dapagliflozin, a selective SGLT2 inhibitor, improves glucose homeostasis in normal and diabetic rats, *Diabetes* 57 (6) (2008) 1723–1729.
- [14] H. Oshima, et al., Empagliflozin, an SGLT2 inhibitor, reduced the mortality rate after acute myocardial infarction with modification of cardiac metabolomes and antioxidants in diabetic rats, *J. Pharmacol. Exp. Therapeut.* 368 (3) (2019) 524–534.
- [15] S. Lahnwong, et al., Acute dapagliflozin administration exerts cardioprotective effects in rats with cardiac ischemia/reperfusion injury, *Cardiovasc. Diabetol.* 19 (1) (2020) 91.

- [16] F.F. Ren, et al., Dapagliflozin attenuates pressure overload-induced myocardial remodeling in mice via activating SIRT1 and inhibiting endoplasmic reticulum stress, *Acta Pharmacol. Sin.* 43 (7) (2022) 1721–1732.
- [17] J. Tian, et al., Dapagliflozin alleviates cardiac fibrosis through suppressing EndMT and fibroblast activation via AMPK α /TGF- β /Smad signalling in type 2 diabetic rats, *J. Cell Mol. Med.* 25 (16) (2021) 7642–7659.
- [18] E. Ehler, T. Moore-Morris, S. Lange, Isolation and culture of neonatal mouse cardiomyocytes, *J. Vis. Exp.* (79) (2013).
- [19] F. Lopez-Jimenez, et al., Weight change after myocardial infarction—the enhancing recovery in coronary heart disease patients (ENRICHED) experience, *Am. Heart J.* 155 (3) (2008) 478–484.
- [20] A. Di Franco, et al., Sodium-dependent glucose transporters (SGLT) in human ischemic heart: a new potential pharmacological target, *Int. J. Cardiol.* 243 (2017) 86–90.
- [21] A.B. García-Redondo, et al., NADPH oxidases and vascular remodeling in cardiovascular diseases, *Pharmacol. Res.* 114 (2016) 110–120.
- [22] D. Lv, et al., Tubeimoside I ameliorates myocardial ischemia-reperfusion injury through SIRT3-dependent regulation of oxidative stress and apoptosis, *Oxid. Med. Cell. Longev.* 2021 (2021) 5577019.
- [23] G. Salazar, NADPH oxidases and mitochondria in vascular senescence, *Int. J. Mol. Sci.* 19 (5) (2018).
- [24] L. Rochette, et al., Nitric oxide synthase inhibition and oxidative stress in cardiovascular diseases: possible therapeutic targets? *Pharmacol. Ther.* 140 (3) (2013) 239–257.
- [25] W.A. Villaume, Marginal BH4 deficiencies, iNOS, and self-perpetuating oxidative stress in post-acute sequelae of Covid-19, *Med. Hypotheses* 163 (2022) 110842.
- [26] N. Zamzami, et al., Sequential reduction of mitochondrial transmembrane potential and generation of reactive oxygen species in early programmed cell death, *J. Exp. Med.* 182 (2) (1995) 367–377.
- [27] H.M. Steinman, The Bcl-2 oncoprotein functions as a pro-oxidant, *J. Biol. Chem.* 270 (8) (1995) 3487–3490.
- [28] N. Zamzami, et al., Reduction in mitochondrial potential constitutes an early irreversible step of programmed lymphocyte death in vivo, *J. Exp. Med.* 181 (5) (1995) 1661–1672.
- [29] W. Xu, T. Zhao, H. Xiao, The implication of oxidative stress and AMPK-nrf2 antioxidative signaling in pneumonia pathogenesis, *Front. Endocrinol.* 11 (2020) 400.
- [30] L.A. Gallo, E.M. Wright, V. Vallon, Probing SGLT2 as a therapeutic target for diabetes: basic physiology and consequences, *Diabetes Vasc. Dis. Res.* 12 (2) (2015) 78–89.
- [31] C.M. Oh, et al., Cardioprotective potential of an SGLT2 inhibitor against doxorubicin-induced heart failure, *Korean Circ. J.* 49 (12) (2019) 1183–1195.
- [32] C.G. Santos-Gallego, et al., Empagliflozin ameliorates adverse left ventricular remodeling in nondiabetic heart failure by enhancing myocardial energetics, *J. Am. Coll. Cardiol.* 73 (15) (2019) 1931–1944.
- [33] S.D. Anker, et al., Empagliflozin in heart failure with a preserved ejection fraction, *N. Engl. J. Med.* 385 (16) (2021) 1451–1461.
- [34] S.S. Hansen, E. Aasum, A.D. Hafstad, The role of NADPH oxidases in diabetic cardiomyopathy, *Biochim. Biophys. Acta (BBA) - Mol. Basis Dis.* 1864 (5, Part B) (2018) 1908–1913.
- [35] S. Lu, et al., Hyperglycemia acutely increases cytosolic reactive oxygen species via O-linked GlcNAcylation and CaMKII activation in mouse ventricular myocytes, *Circ. Res.* 126 (10) (2020) e80–e96.
- [36] P.A. MacCarthy, et al., Impaired endothelial regulation of ventricular relaxation in cardiac hypertrophy: role of reactive oxygen species and NADPH oxidase, *Circulation* 104 (24) (2001) 2967–2974.
- [37] Q. Ma, Role of nrf2 in oxidative stress and toxicity, *Annu. Rev. Pharmacol. Toxicol.* 53 (2013) 401–426.
- [38] Q. Zhang, et al., Activation of Nrf2/HO-1 signaling: an important molecular mechanism of herbal medicine in the treatment of atherosclerosis via the protection of vascular endothelial cells from oxidative stress, *J. Adv. Res.* 34 (2021) 43–63.
- [39] I. Bellezza, et al., Nrf2-Keap1 signaling in oxidative and reductive stress, *Biochim. Biophys. Acta Mol. Cell Res.* 1865 (5) (2018) 721–733.
- [40] A.M. Hussein, et al., Comparative study of the effects of GLP1 analog and SGLT2 inhibitor against diabetic cardiomyopathy in type 2 diabetic rats: possible underlying mechanisms, *Biomedicines* 8 (3) (2020) 43.
- [41] D.P. Del Re, et al., Fundamental mechanisms of regulated cell death and implications for heart disease, *Physiol. Rev.* 99 (4) (2019) 1765–1817.
- [42] Q. Zhang, et al., Signaling pathways and targeted therapy for myocardial infarction, *Signal Transduct. Targeted Ther.* 7 (1) (2022) 78.
- [43] Y. Ye, et al., SGLT-2 inhibition with dapagliflozin reduces the activation of the Nlrp3/ASC inflammasome and attenuates the development of diabetic cardiomyopathy in mice with type 2 diabetes. Further augmentation of the effects with saxagliptin, a DPP4 inhibitor, *Cardiovasc. Drugs Ther.* 31 (2) (2017) 119–132.
- [44] R. Chen, et al., SGLT2 inhibitor-pretreated macrophage transplantation improves adverse ventricular remodeling after acute myocardial infarction, *J. Cardiovasc. Pharmacol.* 82 (4) (2023) 287–297.
- [45] J. Zhang, et al., Metformin protects against myocardial ischemia-reperfusion injury and cell pyroptosis via AMPK/NLRP3 inflammasome pathway, *Aging (Albany NY)* 12 (23) (2020) 24270–24287.
- [46] J. Duan, et al., Protective effect of butin against ischemia/reperfusion-induced myocardial injury in diabetic mice: involvement of the AMPK/GSK-3 β /Nrf2 signaling pathway, *Sci. Rep.* 7 (2017) 41491.
- [47] Q. Luo, et al., mtROS-mediated Akt/AMPK/mTOR pathway was involved in Copper-induced autophagy and it attenuates Copper-induced apoptosis in RAW264.7 mouse monocytes, *Redox Biol.* 41 (2021) 101912.